Synthesis, In Vitro Receptor Binding, and In Vivo Evaluation of Fluorescein and Carbocyanine Peptide-Based Optical Contrast Agents

Samuel Achilefu,*,† Hermo N. Jimenez,‡ Richard B. Dorshow,‡ Joseph E. Bugaj,‡ Elizabeth G. Webb,‡ R. Randy Wilhelm,‡ Raghavan Rajagopalan,‡ Jill Johler,‡ and Jack L. Erion‡

Mallinckrodt Institute of Radiology, Washington University School of Medicine, 4525 Scott Avenue, St. Louis, Missouri 63110, and Mallinckrodt Inc., 675 McDonnell Boulevard, St. Louis, Missouri 63042

Site-specific delivery of drugs and contrast agents to tumors protects normal tissues from the cytotoxic effects of drugs and enhances the contrast between normal and pathologic tissues. One approach to achieve selectivity is to target overexpressed receptors on the membranes of tumor cells and to visualize the tumors by a noninvasive optical imaging method. Accordingly, we conjugated fluorescein and carbocyanine dyes to somatostatin and bombesin receptor-avid peptides and examined their receptor binding affinities. We also prepared potential dual imaging probes consisting of a bioactive peptide for tumor targeting, a biocompatible dye for optical imaging, and a radioactive or paramagnetic metal chelator for scintigraphic or magnetic resonance imaging of tumors. Using these approaches, the resulting carbocyanine derivatives of somatostatin and bombesin analogues retained high binding for their respective receptors. Further evaluation of representative molecules in rats bearing somatostatin- and bombesin-positive tumors showed selective uptake of the agents by the tumor cells. Unlike carbocyanine derivatives, the receptor binding of fluorescein−somatostatin peptide conjugates was highly sensitive to the type of linker and the site of fluorescein attachment on the nonreceptor binding region of the peptide. In general, the presence of flexible linkers disrupted binding affinity, possibly due to the interaction of the linker's thiourea group with the peptide's cyclic disulfide bond. While the receptor binding affinity of the dual probes was not dependent on the type of chelating group examined, it was affected by the relative positions of fluorescein and chelator on the lysine linker. For somatostatin compounds, best results were obtained when the chelator was on the α-amino lysine linker and fluorescein was on the ε-amino group. In contrast, conjugation of the chelator to ε- and fluorescein to the α-amino lysine linker of bombesin peptides resulted in high receptor binding. These findings indicate that despite their small size, conjugation of dyes to truncated somatostatin and bombesin peptide analogues results in promising diagnostic agents that retain high receptor binding activity in vitro. The results further show that these contrast agents can selectively and specifically localize in receptor-positive tumors in rat models.

Introduction

Biomedical optical imaging is an emerging diagnostic method that uses propagating light to activate chromophores in tissues and a detector to capture the transmitted or reflected photons.[1,2] It provides distinctly new diagnostic capabilities while complementing conventional imaging modalities.[3−7] Previous studies have demonstrated the feasibility of using endogenous contrast effectors such as the ratio of oxy- and deoxyhemoglobin to detect pathologic tissues by optical imaging and spectroscopy in the visible and near-infrared (NIR) wavelengths.[1,8] This approach represents a viable, noninvasive method to monitor various diseased states, quantify pathologically relevant physiologic functions, and localize cancer. However, delineation of the spectral differences between normal and pathologic tissues based on endogenous contrast, especially at the early stages of cancer, remains difficult despite the availability of sophisticated image reconstruction algorithms.[9−15] For this reason, several studies are currently focusing on the use of exogenous optical contrast agents to improve image resolution by increasing the signal-to-noise ratio. Unlike endogenous contrast effectors, these compounds are less dependent on inter- and intraspecies variations and can furnish unique information regarding the functional status of tissues. These agents also promote rapid selective localization, improve specificity and sensitivity, and provide important histopathological information such as cell viability.

The utility of contrast agents in diagnostic procedures depends on the preferential accumulation of the molecules in target tissues. One approach to achieve this selectivity in oncology takes advantage of the overexpression of specific receptors on certain tumor cells to target various diagnostic agents to tumors.[16] Hence, a useful strategy involves conjugating a contrast agent to carriers that target the overexpressed tumor receptors to enhance specificity, as demonstrated with fluorescein− and carbocyanine−antibody conjugates.[17−24] Beside antibodies, dye conjugation to other large targeting molecules, which are occasionally coupled by secondary activation mechanisms, also enhances site-

* To whom correspondence should be addressed. Tel.: 314-362-8599. Fax: 314-747-5191. E-mail: achilefu@mir.wustl.edu.
† Washington University School of Medicine.
‡ Mallinckrodt Inc.

specific delivery of the agents.[25,26] However, targeting of tumor receptors with antibodies or large biomolecules is hampered by many factors, including low diffusion rates into tumors, rapid uptake by the liver, and the potential to elicit adverse immunogenic reactions.

On the basis of previous findings that somatostatin and bombesin receptors are up-regulated on many tumor cell membranes and that truncated peptide analogues of the native ligands effectively target these receptors, we recently demonstrated for the first time that this approach is applicable to optical imaging of tumors.[27] The bioconjugates selectively localized in somatostatin-positive tumors without loss of the probe's photophysical properties. More recently, other studies have supported this finding.[28,29] Some advantages of the peptide-based approach include enhanced localization in tumors, rapid clearance from nontarget tissues, ease of structure—activity relationship studies, and the possibility of preparing a combinatorial library of peptides for rapid identification of bioactive molecules.

Earlier reports in nuclear medicine have demonstrated that in vitro receptor binding studies with somatostatin and bombesin peptide analogues correlate with in vivo findings.[30-35] As progress in the design of novel receptor-based optical contrast agents continues, the need exists for rapid screening of these compounds by quantifying their receptor binding affinity. Accordingly, we report here the preparation and biological evaluation of novel, peptide-based receptor-specific optical contrast agents that absorb and emit radiation in the visible (fluorescein derivatives) and the NIR (carbocyanine derivatives) regions. Both fluorescein and carbocyanine dye-labeled biomolecules are widely used in optical imaging studies. Because of the rapid attenuation of light by endogenous chromophores in the visible wavelength (400—700 nm), the fluorescein derivatives are useful for imaging superficial lesions, endoscopy-accessible deep tissues, surgically exposed tissues, and delicate organs such as the prostate, where rapid attenuation of light prevents damage to sensitive organ parenchymal cells. At the NIR region between 700 and 900 nm, the low light scattering and absorption by endogenous photoactive biomolecules permit photons to penetrate several centimeters into tissue. Thus, the carbocyanine dye derivatives are particularly useful for detecting and diagnosing pathologic conditions in deep tissues.

Furthermore, optical imaging is an emerging diagnostic method and its acceptance in clinical practice requires validation of the images obtained with established imaging modalities such as scintigraphy and magnetic resonance imaging (MRI).[6,36-38] One approach to validating optical imaging involves the coregistration of the target tissue with a second modality using the same exogenous contrast molecule. To this effect, we synthesized and evaluated novel dual imaging probes comprising a receptor-avid peptide for tumor targeting, fluorescein for optical imaging, and a radioactive or paramagnetic metal chelator for scintigraphy or MRI, respectively. This method would obviate the need to administer two or more different compounds that may complicate the coregistration due to differences in the individual drug's pharmacokinetics.

Chemistry

Fluorescein Isothiocyanate (FITC) Derivatives. We prepared four groups of fluorescein-labeled peptides as shown in Tables 1—4. Previous studies have demonstrated that the truncated somatostatin and bombesin octapeptides **2** and **13** exhibit high binding to their appropriate receptors.[32,39] Consequently, we retained the basic structural framework of these peptides in all somatostatin and bombesin derivatives prepared. The peptides were synthesized on solid support by standard automated fluorenylmethyloxycarbonyl (Fmoc) solid phase synthesis.[40] Subsequent conjugation of commercially available FITC with the peptides was performed either on solid support or by solution phase synthesis, depending on the nature of the peptide.

Fluorescein derivatives of peptides devoid of multiple FITC-reactive functional groups, such as **17**, are readily prepared by solution phase reaction, while those possessing more than one FITC-reactive site on cleavage from the resin, such as **3**, are best prepared on solid phase before removing all side chain protecting groups. However, reaction of FITC with **2** to form **3** on solid support was slow and gave poor yields (<5%) of the desired isolated compound. We also observed a similar trend for all of the peptides possessing N-terminal aromatic amino acid units, and this low yield could be attributed to steric factors. Hence, we investigated the traditional solution phase reaction for the conjugation of FITC to the somatostatin peptide analogues. Initially, we prepared the octapeptide (**2**) on trityl resins, which permits cleavage of the peptide from the solid support with mild acids that leave all side chain protecting groups intact. Selective removal of the N-terminal Fmoc protecting group, followed by base-catalyzed coupling of FITC in solution, did not give the desired compound after high-performance liquid chromatography (HPLC) separation of the crude mixture. It is possible that the bulky side chain protecting groups hinder the reaction of FITC with amines under this reaction condition. Because the reactivity of FITC favors primary amines, we overcame this problem by removing all side chain protecting groups, except the K^5 ϵ-amino group that is critical for maintaining the peptide's receptor binding activity. The orthogonal protecting group was removed after conjugation of fluorescein to the N-terminal amino group (Scheme 1). This approach consistently gave the desired compounds shown in Table 1. However, we observed that the introduction of hydrophilic and lipophilic spacers to the nonreceptor binding N-terminal end of the somatostatin peptide enhanced the conjugation of FITC to the peptide on solid support.

Synthesis of the fluorescein derivatives of bombesin peptide analogues was readily accomplished by solution phase reaction since the receptor binding moiety does not contain multiple FITC-reactive functions (Table 3). Selective attachment of FITC to the α- or ϵ-amino group of lysine was accomplished by orthogonal protection of the amines with either Fmoc or 1-(4,4-dimethyl-2,6-dioxocyclohexylidene)-3-methylbutyl) (ivDde) group. Typically, the amino group for FITC attachment is protected as Fmoc to enable automatic deprotection of the amino group by standard peptide synthesis protocol. For the synthesis of homogeneous dual optical probes (**20** and **24**), both amino functions of lysine were protected with

Scheme 1

dF-C-Y(*t*Bu)-dW(Boc)-K(Dde)-T(*t*Bu)-C-T(*t*Bu)-**Resin**
| |
S————————————————————S

Cleavage (trityl resin)   (i) Cleavage (ii) Partial deprotection (Wang Resin)

dF-C-Y(*t*Bu)-dW(Boc)-K(Dde)-T(*t*Bu)-C-T(*t*Bu)-OH   dF-C-Y-dW-K(Dde)-T-C-T-OH
| | | |
S————————————————S   S——————S

(i) FITC (ii) Deprotection ✕   (i)FITC (ii) H_2NNH_2

FITC-dF-C-Y-dW-K-T-C-T-OH
| |
S——————S

Table 1. Somatostatin Analogues and Fluorescein Derivatives

Compd	Condensed Structure[a]	IC_{50} (nM)	SE ± (nM)
1	dF-C-Y-dW-K-T-C-T-ol S————S	0.4	0.07
2	dF-C-Y-dW-K-T-C-T-OH S————S	0.6	0.10
3	FITC-dF-C-Y-dW-K-T-C-T-OH S————S	9.9	2.1
4	FITC-βA-dF-C-Y-dW-K-T-C-T-OH S————S	>1,000	NA[b]
5	FITC-G-S-G-dF-C-Y-dW-K-T-C-T-OH S————S	285.2	NA
6	α-FITC-K-dF-C-Y-dW-K-T-C-T-OH S————S	6.4	1.3
7	ε-FITC-K-dF-C-Y-dW-K-T-C-T-OH S————S	187.8	NA

a FITC, fluorescein thiourea group; T-ol, threoninol; T-OH, threonine. *b* NA, not applicable because our assay was limited to 100 nM of the competing ligand and the stated IC_{50} value was obtained by extrapolating the data from a four parameter curve-fitting program.

Table 2. Somatostatin Analogues for Multimodality Imaging

Compd	Condensed Structure[a]	IC_{50} (nM)	SE ± (nM)
8	DTPA-dF-C-Y-dW-K-T-C-T-OH S————S	1.9	0.2
9	(α-DTPA-ε-FITC)-K-dF-C-Y-dW-K-T-C-T-OH S————S	10.3	1.8
10	(α-FITC-ε-DTPA)-K-dF-C-Y-dW-K-T-C-T-OH S————S	71.3	NA
11	(α-DOTA-ε-FITC)-K-dF-C-Y-dW-K-T-C-T-OH S————S	10.3	2.1

a FITC, fluorescein thiourea group.

identical groups (usually Fmoc) during peptide synthesis. Expectedly, solid and solution phase reactions of FITC with **14** and **16** gave a mixture of the bis-fluorescein derivatives (**20** and **24**) and the corresponding α- and ε-amino lysine mono-FITC analogues. Fortunately, the differences in the retention time of each

compound on HPLC are sufficient to facilitate their isolation with ease. While the mono- and bis-FITC derivatives are readily distinguishable by mass spectrometry, the isomeric monoderivatives were identified by spiking each fraction of the isolated compounds with authentic samples prepared by the orthogonal protection procedure described above. Because of the simplicity of this reaction procedure and the ease of isolating each component of the reaction product, we also used this one pot synthesis approach for the preparation of all three (α-, ε-, and bis-fluorescein) derivatives.

The tandem receptor-specific dye−chelator probes prepared for potential dual optical and scintigraphic or MRI are shown in Tables 2 and 4. The availability of chelator precursors that are compatible with solid phase synthesis[41] allowed us to prepare the diethylenetriaminepentaacetic acid (DTPA) and cyclododecane-1,4,7,-10-tetraazaacetic acid (DOTA) derivatives on solid support. Thus, in all cases, we coupled orthogonally protected tri-*tert*-butyl DTPA or tri-*tert*-butyl DOTA to an α- or ε-amino group of lysine by the same automated solid phase synthesis procedure used to prepare the peptides.[41] Although direct coupling of FITC to the chelator−peptide derivatives on solid support was not successful, good results were obtained by solution phase reactions. For the somatostatin tandem probes (Table 2), the K^6 ε-amino group was protected with ivDde, the α- or ε-amino function of K^1 for coupling the chelator was protected with Fmoc, and the remaining K^1 amino group for FITC attachment was protected with a *tert*-butyloxycarbonyyl (Boc) group. Cleavage of the chelator−peptide derivative from the resin also removes the Boc protection, and reaction of FITC with this free amine, followed by removal of the ivDde group, gave the desired compounds **9**−**11**. Because the bombesin peptide analogues in Table 4 lack multiple FITC-reactive groups, the synthesis of compounds **29**−**31** involves concomitant cleavage of the peptide from the resin and removal of all side chain protecting groups, followed by coupling of FITC to the peptide.

Carbocyanine Derivatives. The receptor-specific carbocyanine derivatives prepared for this study absorb and fluoresce in the NIR region and are thus useful for deep tissue imaging. Scheme 2 summarizes the procedure employed to prepare the NIR optical probes shown in Table 5. Synthesis of the carbocyanine dyes has been described elsewhere.[27,29] All other reactions, including

Table 3. Bombesin Analogues and Fluorescein Derivatives

compd	condensed structure[a]	IC$_{50}$ (nM)	SE $\pm$ (nM)
12	pQ-Q-R-Y-G-N-Q-W-A-V-G-H-L-M-NH$_2$	1.1	0.2
13	Q-W-A-V-G-H-L-M-NH$_2$	28.3	3.7
14	K-Q-W-A-V-G-H-L-M-NH$_2$	10.5	3.8
15	G-S-G-Q-W-A-V-G-H-L-M-NH$_2$	7.6	1.3
16	K-G-S-G-Q-W-A-V-G-H-L-M-NH$_2$	4.8	0.6
17	FITC-Q-W-A-V-G-H-L-M-NH$_2$	3.2	0.4
18	α-FITC-K-Q-W-A-V-G-H-L-M-NH$_2$	5.8	1.4
19	ε-FITC-K-Q-W-A-V-G-H-L-M-NH$_2$	5.7	1.5
20	α,ε-(FITC)$_2$-K-Q-W-A-V-G-H-L-M-NH$_2$	9.5	1.8
21	FITC-G-S-G-Q-W-A-V-G-H-L-M-NH$_2$	9.2	0.3
22	α-FITC-K- G-S-G-Q-W-A-V-G-H-L-M-NH$_2$	15.6	4.8
23	ε-FITC-K-G-S-G-Q-W-A-V-G-H-L-M-NH$_2$	9.6	1.7
24	α,ε-(FITC)$_2$-K G-S-G-Q-W-A-V-G-H-L-M-NH$_2$	20.5	2.9

[a] FITC, fluorescein thiourea group; pQ, pyroglutamic acid.

Table 4. Bombesin Analogues for Multimodality Imaging

compd	condensed structure[a]	IC$_{50}$ (nM)	SE $\pm$ (nM)
25	DTPA-P-Q-R-Y-G-N-Q-W-A-V-G-H-L-M-NH$_2$	4.7	0.3
26	α-DTPA-K-Q-W-A-V-G-H-L-M-NH$_2$	410	NA
27	ε-DTPA-K-Q-W-A-V-G-H-L-M-NH$_2$	4.8	1.1
28	α,ε-(DTPA)$_2$-K-Q-W-A-V-G-H-L-M-NH$_2$	240	NA
29	α-DTPA-ε-FITC-K-Q-W-A-V-G-H-L-M-NH$_2$	276	NA
30	α-FITC-ε-DTPA-K-Q-W-A-V-G-H-L-M-NH$_2$	20	11.7[b]
31	α-FITC-ε-DOTA-K-Q-W-A-V-G-H-L-M-NH$_2$	15	9[b]

[a] FITC, fluorescein thiourea group. [b] The shape of the competitive binding curves for these compounds does not conform to regular inhibition curve form, despite repeated experiments. Receptor binding assay was optimized for IC$_{50}$ values between 1 and 10 nM.

Scheme 2
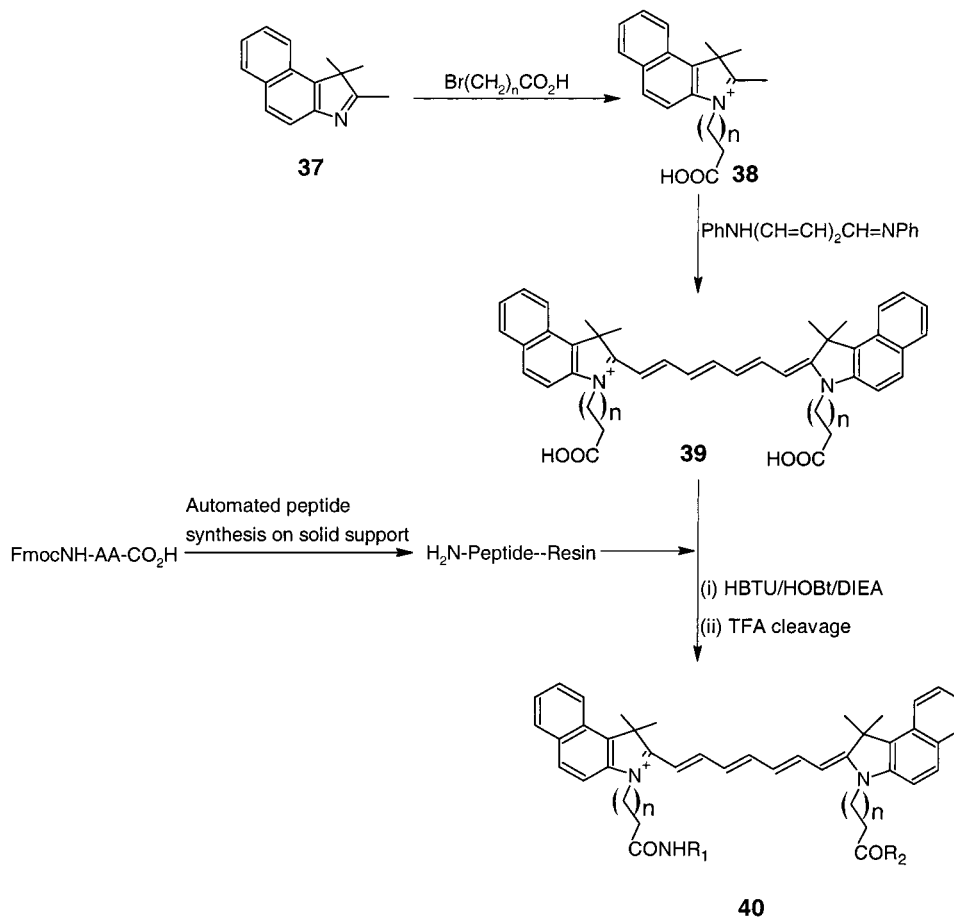
conjugation of the dye to peptides, were carried out on solid support. This approach enabled us to selectively prepare the monopeptide conjugates and a mixture of the mono band the bis-peptide derivatives, depending on the reaction conditions. Activation of carbocyanine bis-

propanoic acid (**39**) with 3 equiv of a carboxyl-activating reagent and subsequent condensation to the N terminus amino group of **2** gave predominantly the monooctapeptide conjugate (**32**). A significant amount of the bis-peptide derivative can be prepared by reactivating the

Table 5. Pepde-Carbocyanine NIR Optical Contrast Agents

Compd	Receptor	R_1	R_2	n	IC_{50} (nM)	SE ± (nM)
32	Somatostatin	-dF-C-Y-dW-K-T-C-T-OH S————S	OH	1	4.6	0.7
33	Somatostatin	-dF-C-Y-dW-K-T-C-T-OH S————S	OH	4	5.4	1.0
34	Somatostatin	-dF-C-Y-dW-K-T-C-T-OH S————S	NHR_1	4	1.1	0.1
35	Somatostatin	-βA-dF-C-Y-dW-K-T-C-T-OH S————S	OH	1	3.4	0.4
36	Bombesin	-G-S-G-Q-W-A-V-G-H-L-M-NH₂	OH	1	1.8	0.2

free carboxylic acid group of the monopeptide—carbocyanine dye while still on solid support and allowing the reaction to proceed for 24 h in the dark. Elongation of the *N*-alkyl group of the carbocyanine dye from ethyl (**40**, $n = 1$) to pentyl (**40**, $n = 4$) facilitated the preparation of both mono- (**33**) and bis- (**34**) peptide derivatives with 3 equiv of a carboxyl activation reagent. Isolation of these compounds by HPLC was not cumbersome due to the large difference in the elution pattern of the mono- and bis-peptide derivatives, as described in the Experimental Section.

The absorption and emission of fluorescein (λ_{max} 490 nm absorption, 530 nm emission), carbocyanine dye **39** (λ_{max} 795 absorption, 830 emission), and their respective bioconjugates in 25% aqueous dimethyl sulfoxide (DMSO) were practically the same at the submicromolar concentrations examined. At higher concentrations (100 μM), changes in photophysical properties of the dyes arise from molecular aggregation or dimerization.[42]

Biological Results and Discussion

In Vitro Studies. Results of the in vitro binding assays of fluorescein derivatives are shown in Tables 1 and 2 for somatostatin receptor using the rat pancreatic tumor cell line, CA20498, and Tables 3 and 4 for bombesin receptor using the rat pancreatic acinar cell line, AR42-J. Table 5 shows the receptor binding affinity of the carbocyanine derivatives for both somatostatin and bombesin receptors. Both tumor cell lines express somatostatin and bombesin receptors. Established somatostatin or bombesin receptor-avid peptides were used as internal standard for the receptor binding studies. To validate the assay, we assessed the binding of fluorescein disodium salt, indocyanine green, and the carbocyanine dye **39**, all of which are devoid of a receptor-avid peptide component. No binding to receptors was observed in the presence of up to 100 nM concentration of these dyes, and similar results were obtained with scrambled peptides that lack the receptor binding motif (Figure 1). The reliability of the assay protocol was also confirmed by the lack of competitive inhibition of a radiolabeled bombesin receptor-avid

Figure 1. Inhibition of [¹¹¹In]-DTPA-[Y⁴]-bombesin (trace) binding to AR42-J membranes using varying concentrations of control compounds and known competitors. Symbols correspond to the following compounds: ◇, DTPA-[Y4]-bombesin; ●, bombesin; ○, FITC; ■, ICG; □, cypate.

Figure 2. Inhibition of [¹¹¹In]-DTPA-[Y⁴]-bombesin (trace) binding to AR42-J membranes using varying concentrations of the bombesin analogues listed in Table 3. Symbols corresponding to compounds or to number codes given in Table 3 are as follows: ○, DTPA-[Y⁴]-bombesin; ●, **14**; □, **15**; ■, **16**; ◇, **17**; ◆, **18**; △, **19**; ▲, **20**; ▽, **21**; ▼, **22**.

tracer by an otherwise somatostatin receptor-avid dye-labeled peptide.

After we established the reliability of the binding assays, we evaluated the receptor binding affinity of the novel compounds prepared. Most of the new compounds effectively competed with the receptor binding of the appropriate reference standard (Figures 2 and 3). As shown in Table 1, direct coupling of FITC to the bioactive somatostatin octapeptide **2** to form **3** resulted in a peptide with high receptor affinity, having an IC_{50} in the nanomolar range. We further investigated the effect of linkers at the nonreceptor binding N terminus that could improve the peptide's solubility in a biological medium, modify the in vivo biodistribution, and facilitate the preparation of tandem heterogeneous diagnostic probes for combined optical and scintigraphic or magnetic resonance tumor imaging. Introduction of a non-bulky hydrophobic linker was expected to minimize the renal excretion of **2** and enhance the conjugation of FITC to peptides on solid support. However, coupling of β-alanine to **2** and subsequent conjugation of FITC to obtain **4** drastically reduced the binding affinity (IC_{50} > 1 μM). Compound **5**, which has a hydrophilic linker between FITC and **2**, improved water solubility and receptor binding as compared with **4**, albeit still orders of magnitude lower than **3**. Addition of a lysine linker to **2** provides two sites for coupling one or more probes

Figure 3. Inhibition of [^{111}In]-DTPA-[Y^3]-octreotate (trace) binding to CA20948 membranes using varying concentrations of the somatostatin analogues listed in Table 1. Symbols corresponding to compounds or to number codes given in Table 1 are as follows: ○, DTPA-[Y^3]-octreotate; ●, **1**; □, **2**; ■, **3**; ◇, **4**; ◆, **6**; ▽, **5**.

to the same molecule. Of these possible positions, conjugation of FITC to the α-amino lysine group (**6**) is preferred to the ε-position (**7**).

The inclusion of a lysine linker enabled us to prepare molecules that are potentially useful for diagnosis of tumors by a dual imaging system. This approach could provide distinctly new diagnostic information while complementing established imaging modalities. Because optical tomography is an emerging diagnostic method, tandem probes are also useful for cross-validation purposes. Accordingly, we coupled FITC and a chelator to the alternate amino group of the nonbinding N-terminal lysine (Table 2). We chose DTPA and DOTA as chelators because they are widely used to prepare radioactive and paramagnetic metal chelates for biomedical imaging.[41,43,44] Table 2 shows that while the relative position of the metal chelator and optical probe affect the receptor binding affinity of the peptides, the nature of the chelating group (linear DTPA or cyclic DOTA) had virtually no effect. Thus, for such dual heterogeneous imaging agents, coupling the chelator to the α-position and the optical probe to the ε-position of lysine resulted in conjugates that retain the receptor binding affinity of the peptide.

Similarly, we evaluated the binding affinity of several derivatives of bombesin receptor-avid peptides. Unlike somatostatin analogues, all of the bombesin peptide derivatives had high receptor affinity with measured IC$_{50}$ values in the nanomolar range, indicating tolerance of the N terminus modifications by the peptide's pharmacophore (Table 3). However, as with the somatostatin analogues, the receptor binding affinity of the dual probes was less dependent on the nature of the chelator (**30** and **31**) but was affected by the relative position of the optical probe and the chelator (**29** and **30**). In this case, the preferred molecular design requires coupling the chelator to the ε-amino group and the optical probe to the nonreceptor binding α-amino lysine position.

All of the NIR-absorbing carbocyanine dye derivatives prepared, which are useful for deep tissue optical imaging, retained very high binding affinity for somatostatin and bombesin receptors (Table 5). Within the somatostatin series, increasing the dye's linker *N*-alkyl chain length from ethyl (**32**) to pentyl (**33**) or the introduction of a β-alanine spacer (**35**) did not consider-

ably alter the receptor binding affinity of these compounds. However, comparison of **32** and **34** shows that the bis-peptide derivative **34** has about four times the receptor binding affinity of the monopeptide conjugate **32**. This difference in binding could be attributed to cooperative effect of the two peptides per dye molecule. In the case of carbocyanine−bombesin conjugate **36**, higher receptor binding affinity than the parent peptide **15** was obtained.

In Vivo Studies. Whole body imaging of rats and imaging of excised organs were accomplished by using a low-powered continuous wave laser source to excite the probe at the appropriate wavelength and monitor the distribution of the imaging agent with a charge-coupled device camera. The characteristic absorption (490 nm) and fluorescence (530 nm) of fluorescein require the use of light in the visible region for optimal localization of pathologic tissues with the aid of fluorescein-based contrast agent. Hence, fluorescein derivatives are best-suited for imaging superficial tissues because of the shallow penetration of blue light in tissues. In contrast, the absorption (780 nm) and fluorescence (830 nm) of the carbocyanine derivatives in the NIR region permit their use for optical imaging of deep tissues.

For in vivo optical imaging, we injected AR42-J (bombesin receptor-positive) or CA20948 (somatostatin receptor-positive) pancreatic tumor cells into the left flank of rats and allowed them to grow into a palpable mass. Control experiments with inactive receptor binding fluorescein disodium salt and the low-receptor affinity β-alanine-somatostatin fluorescein derivative (**4**) show that these compounds were not retained in the tumor.

A representative fluorescein-based somatostatin receptor binding peptide **3** was injected into the lateral tail vein of CA20948 tumor-bearing rats. Preferential retention of the agent in the tumor was slow and peaked at about 1 h postinjection but remained in the tumor up to 5 h later (Figure 4). On the other hand, differentiation of the tumor from normal tissue was evident 10 min postinjection of the bombesin peptide analogue **17** into AR42-J tumor-bearing rats. Although time sequence imaging showed that the preferential retention of **17** in the tumor increased gradually with time, this agent cleared from the tumor and other tissues 1 h postinjection. To account for the rapid elimination from tissues, we collected urine and excised various organs and tissue samples 2 h postinjection of **17** into AR42-J tumor-bearing rats. Optical imaging revealed that the conjugate was almost exclusively excreted by the kidneys into urine (Figure 5). Postulating that inhibition of this clearance pathway would improve tumor retention by keeping the probe in blood for a longer period, we carried out a bilateral ligation of the kidneys before injection of **17**. Our results indicate that instead of increasing the tumor retention, the probe reverted to the hepatobilliary excretion route (Figure 5). Thus, despite their favorable receptor binding values, the pharmacokinetics of compounds such as **17** may preclude their use for in vivo tumor detection.

As demonstrated by the in vitro data, the NIR conjugates have high receptor binding affinity. Prior to in vivo evaluation of representative receptor-specific
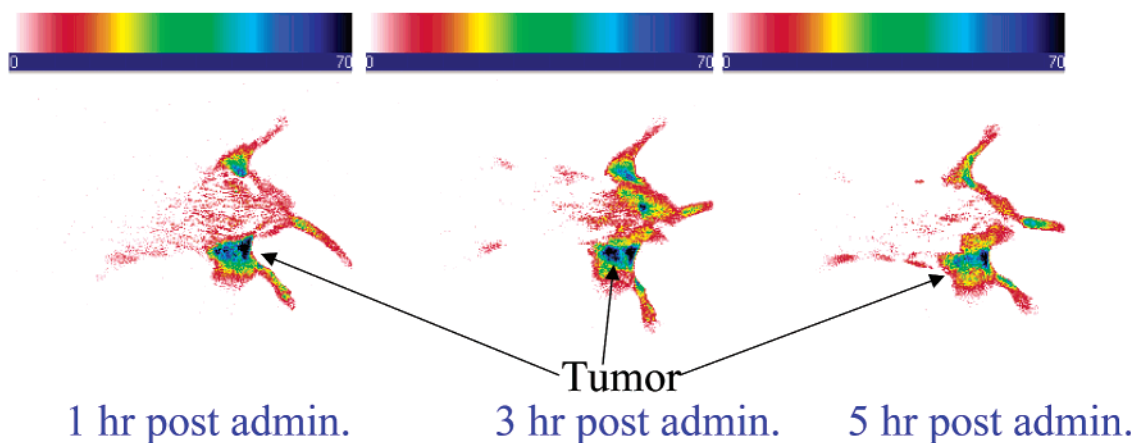
Figure 4. Time sequence localization of fluorescein−somatostatin receptor-avid optical probe **3** in a CA20948 tumor-bearing rat.
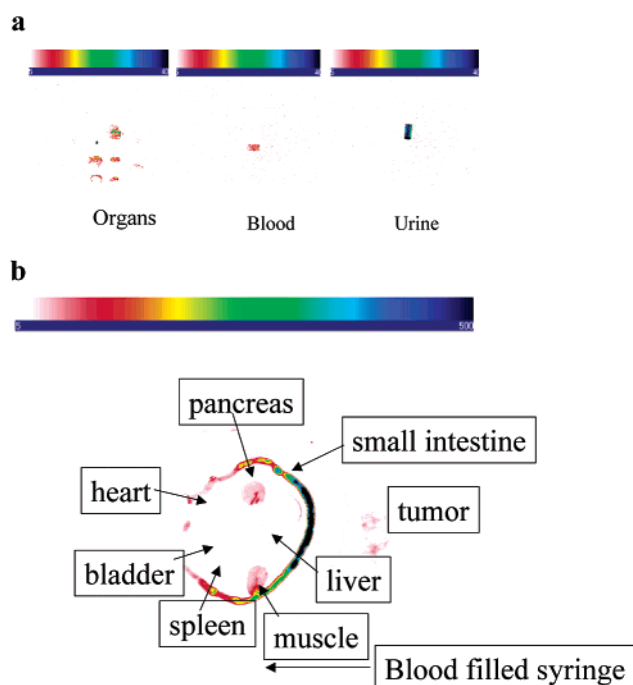
Figure 5. (a) Imaging of urine, excised organs, and tissues 2 h postinjection of **17** to Ar42-J tumor-bearing rat. The organs include liver, pancreas, kidneys, and the heart. The compound is almost exclusively excreted by the kidneys into urine. (b) Imaging of excised organs and tissues 2 h postinjection of **17** into a bilateral ligation of the kidneys of AR42-J tumor-bearing rat. The excretion route changed from renal to hepatobiliary.

Figure 6. (a) Fluorescent image of the NIR somatostatin receptor-avid optical probe **32** in a CA20948 tumor-bearing rat at 27 h postinjection. (b) Fluorescent image of the NIR bombesin receptor-avid optical probe **36** in an AR-42-J tumor-bearing rat at 22 h postinjection.

agents, we assessed the nonspecific retention of the nonconjugated carbocyanine dye **39** in CA20948 tumor-bearing rats. Administration of **39** to tumor-bearing rats, and subsequent time sequence optical imaging, demonstrated that this dye was not retained in the tumor. Furthermore, ex vivo evaluation of excised organs 1 h postinjection showed that the compound was predominantly taken up by the liver. This lack of uptake by the tumor agrees with the observed poor specific binding of the dye to somatostatin receptor. Conversely, the high receptor binding affinity of the carbocyanine−peptide conjugates **32**, **34**, and **36** correlated with selective retention of the agents in tumors in vivo. Time sequence imaging of the whole rat revealed rapid delineation of the tumor within 30 min postinjection and showed that the compounds were retained in tumors

up to 40 h later (Figure 6). The imaging of excised organ parts also confirmed the whole animal imaging results (Figure 7).

Discussion

The upregulation of somatostatin and bombesin receptors in tumors relative to normal surrounding tissues permits the preferential delivery of therapeutic and diagnostic molecules to pathologic cells without harming healthy tissues.[31,35] Previous studies with radiolabeled octapeptide analogues of native somatostatin and bombesin polypeptides demonstrated the site-specific localization of these truncated peptides in the appropriate receptor-positive tumor cells.[44,45] Findings of these studies also showed a good correlation between in vitro receptor binding affinities and selective retention of the peptide's radioactive metal complexes in tumors in vivo.
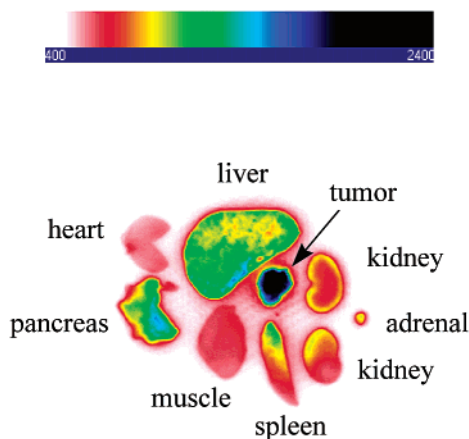
Figure 7. Localization of **32** in tissues of a CA20948 tumor-bearing rat 24 h postadministration.

Consequently, we prepared fluorescein- and carbocyanine-labeled analogues of the truncated somatostatin and bombesin peptides and evaluated their receptor binding activities.

Fluorescein Derivatives. Direct conjugation of FITC to **2** gave the octapeptide **3**, which retained the receptor binding affinity of the ligand in the nanomolar range. However, the difficulty in preparing **3** on solid support and the need to modify the biodistribution of the agent and introduce multiple probes per targeting moiety prompted us to study the effect of both hydrophilic and lipophilic linkers. Although the incorporation of β-alanine to **2** facilitated the synthesis of **4** on solid support, the resulting compound was inactive up to 1 μM. Furthermore, in vivo evaluation of **4** in CA20948 tumor-bearing rats showed no preferential retention in the tumor and was primarily excreted by the kidneys. It is possible that the flexible ethylene linker of β-alanine favored a disruptive interaction of the conjugate's thiourea moiety with the peptide's cyclic disulfide bond. Because the disulfide bond of **4** is critical for the peptide's bioactivity, any such intramolecular interaction could disrupt the receptor binding of the entire molecule. Another plausible explanation for the inactivity of **4** could result from other inhibitory interactions of the hydrophilic fluorescein with the receptor binding domain, which could be induced by the presence of nonsterically hindered flexible linkers such as an ethylene group.

Replacement of the β-alanine with a less flexible nonionic hydrophilic linker to give **5** improved receptor binding, albeit still several orders of magnitude less than **3**. However, substitution of β-alanine in **4** by lysine improved the receptor binding and also provided two possible FITC-reactive sites that influence the bioactivity of the conjugate. Thus, coupling FITC to the α-amino position of lysine gives a compound (**6**) that is several orders of magnitude more active than the ε-amino conjugate analogue (**7**). As expected, attachment of FITC to the flexible ε-amino group increased the potential of the resulting thiourea group to interact with the peptide's disulfide bond or the receptor in a similar manner as was observed with β-alanine (**4**) and GSG (**5**) linkers. However, the extent of this negative interaction appears to depend on the distance of the FITC-reactive site of the flexible linker from the peptide's disulfide bond. Thus, the receptor binding affinity

increased as longer flexible lingers were used (i.e., ε-amino lysine > GSG > β-alanine). Interestingly, direct coupling or conjugation of FITC to a more rigid linker that minimizes interaction of the thiourea group with the peptide's disulfide bond favored high receptor binding of the fluorescein−peptide derivatives such as **3** and **6**. The negative effect of flexible linkers on ligand−receptor binding was only observed in the fluorescein conjugates of the cyclic disulfide somatostatin peptide analogues but not with the bombesin peptide analogues **21**−**23** or the hydrophobic carbocyanine analogue **35**, which retained their receptor binding activity in the presence of flexible linkers.

The influence of fluorescein and linkers on the bioactivity of bombesin peptide analogues is less pronounced relative to somatostatin derivatives (Table 3). Direct attachment of FITC to the bombesin peptide **13** to give **17** improved the receptor binding affinity of the ligand. Furthermore, incorporation of two fluorescein moieties to truncated bombesin peptides did not compromise the receptor binding affinity of the conjugates (**20** and **24**). These homogeneous multiprobe ligands could improve detection sensitivity by a net enhancement of optical signal per molecule and could be particularly useful for imaging tissues with low receptor density. Because bombesin analogues tolerate a variety of substituents at the N terminus without loss of receptor binding activity, they could serve as model bioactive molecules for multispectral optical imaging studies.

Although biomedical optical imaging is not new, recent advances in laser technology and image reconstruction techniques have reignited interest in the use of this highly sensitive and noninvasive method for diagnosing pathologic conditions.[46] Acceptance of optical tomography in clinical settings, however, requires validation of the images with conventional imaging methods such as scintigraphy or MRI. Such cross-validation studies would benefit from the use of a single molecule that is capable of providing important diagnostic information from both optical and other imaging methods. Accordingly, we prepared and evaluated the binding affinity of potential tandem imaging agents (Tables 2 and 4) and compared the result with analogous peptide−chelator conjugates that are traditionally used in nuclear medicine. For example, the DTPA−somatostatin peptide analogue **8** is extensively used in basic research and clinical studies.[47]

On the basis of the somatostatin receptor binding affinity of compounds **6** and **7** (Table 1), we expected that conjugation of FITC to the α-amino lysine and a chelator to the ε-amino group would give better binding molecules than vice versa. To test this hypothesis, we prepared compounds **9** and **10**. The results of binding studies using these molecules were the converse of our expectation (Table 2). Apparently, the relative position of the chelating group to fluorescein significantly influences the receptor binding of the tandem imaging agents. Thus, coupling DTPA to the α-amino group of lysine mitigates the deleterious effect of conjugating FITC to the flexible ε-amino lysine. In addition, changing the chelator from DTPA to DOTA did not alter this result (**10** and **11**). Because the binding affinity of the dual imaging agents was independent of the nature of

the chelating group, initial screening of the somatostatin receptor binding affinity of new dual modality compounds could be accomplished with the less expensive DTPA.

While the receptor binding affinity of various fluorescein−bombesin derivatives showed little variation, incorporation of DTPA into fluorescein-containing bombesin peptides induced a position-dependent binding activity, as was observed with the somatostatin analogues. However, unlike the DTPA−octreotate conjugates (Table 2), coupling DTPA to the ϵ-amino lysine and FITC to the α-amino group improved receptor binding rather than the converse (compare **29** and **30**, Table 4). Replacement of the linear DTPA with DOTA at the ϵ-amino group (**31**) gave a similar receptor binding value. Thus, in designing molecules for tandem fluorescein−chelator probes, the overall activity of the resultant molecule appears to rely on the relative position of the chelator on the linker than fluorescein.

Carbocyanine Derivatives. The carbocyanine derivatives prepared for this study absorb and fluoresce in the NIR region and are thus useful for deep tissue imaging. Coupling the hydrophobic carbocyanine dye **39** to somatostatin and bombesin peptides resulted in conjugates that retained high binding affinity to the appropriate receptor, despite the relatively large size of the dye component. Comparison of the fluorescein and carbocyanine analogues shows that the latter consistently had better receptor binding affinity than the former. Specifically, while the fluorescein conjugate **4** is inactive up to 1 μM, the carbocyanine analogue **35** retained high receptor binding affinity in the nanomolar range. Furthermore, comparison of the carbocyanine− bombesin derivative (**36**, Table 5) with the fluorescein analogue (**21**, Table 3) indicates that the former is about five times better than the latter.

At first glance, the small size of the peptide targeting groups used in this study would suggest that coupling the carbocyanine dye **39**, which is more than twice the molecular weight of fluorescein and constitutes over 40% of the entire conjugate's molecular weight, would interfere with receptor binding. This, however, is not the case. A variety of possible mechanisms could be postulated for the observed high receptor binding of the carbocyanine dye derivatives. It is likely that the large molecular volume of the hydrophobic NIR dye precluded it from fitting into the binding region of the receptor, thereby permitting the bioactive peptide unit to interact exclusively with the receptor. This preclusion of the large hydrophobic dye component could deter competing ligands from displacing the dye−peptide conjugate from the receptor by two possible mechanisms. On one hand, displacement of the receptor-bound peptide of the conjugate by hydrophilic competitors is inhibited by unfavorable interaction by the protruding hydrophobic dye portion. On the other hand, the favorable association of hydrophobic competitors with the dye component prevents access to the receptor binding domain occupied by the peptide component of the conjugate. Both possible mechanisms would enhance the receptor binding of the carbocyanine molecules. However, confirmation of the exact mechanism and the structural disposition of the ligand−receptor interaction would require additional studies beyond the scope of this work.

The in vitro studies also show that while the receptor binding affinity of the carbocyanine conjugates is not influenced by the length of the *N*-alkyl linker, it depends on the number of peptide conjugates per dye molecule (compare **32**−**34**, Table 5). The enhanced receptor binding of the bis-peptide derivative **34** may be attributed to cooperative interaction of the two peptides with the receptor or may be simply due to the effective doubling of the peptides concentration.

Biodistribution and Tumor Localization. The preferential accumulation of the fluorescein conjugate **3** in the somatostatin receptor-positive tumor CA20948 peaked at about 1 h postinjection and suggests active uptake of the compound by the receptor (Figure 4) because in negative control experiments using either fluorescein disodium salt or nonsomatostatin-avid dye− peptide conjugates, retention in the tumor was not observed.

Control experiments with the nonconjugated carbocyanine dye **39** and the corresponding nonsomatostatin-avid peptide conjugates neither localized in the tumor in vivo nor had detectable affinity for the somatostatin receptor in vitro. In contrast, the high receptor binding affinity of the carbocyanine derivatives was also reflected by tumor localization in vivo. Thus, injection of **32** and **34** into somatostatin receptor-positive CA20948 tumor-bearing rat and subsequent optical imaging demonstrates the site-specific localization of the agent in the tumor (Figure 6). Ex vivo imaging of excised organs and tissues shows the predominant retention of the agents in tumor tissues (Figure 7). The small uptake of the agent by the liver and the pancreas is expected because the liver is the primary excretion route of the nonconjugated carbocyanine dye while the rat pancreas possesses some somatostatin receptors. This finding affirms the reliance on the receptor binding studies for rapid evaluation and selection of tumor-specific optical contrast agents for biomedical studies. In addition to its use in tumor diagnosis, this approach is applicable to the treatment of appropriate receptor-positive tumors by a photodynamic therapy method.

In conclusion, we prepared novel optical and heterogeneous dual imaging agents for tumor diagnosis. The delivery mechanism is based on targeting overexpressed receptors on tumor cell membranes. We quantified the receptor binding affinity of all of the reported bioconjugates and showed that the in vitro data correlate positively with the in vivo selective retention of the receptor-specific probes in the appropriate receptor-positive tumor model. The fluorescein and carbocyanine dye conjugates of bombesin peptide analogues retained their receptor binding affinity in the nanomolar range. On the contrary, the receptor binding affinity of the somatostatin receptor-avid optical probes was dependent on the dye used. While the carbocyanine peptide conjugates retained high receptor binding affinity, binding of the fluorescein analogues depended on the nature of the thiourea linker. Conjugation of FITC to form thiourea with an amino group of the peptide via a flexible linker appears to destabilize the peptide's disulfide bond, which is part of the molecule's pharmacophore. Consequently, a more stable fluorescein conjugate of somatostatin peptide analogues may be prepared from fluoresceinamine, which gives an amide

bond that does not destabilize the peptide's disulfide group. Finally, the structural feature of the receptor-specific dual optical-scintigraphic imaging agents represents a new direction toward the validation of clinical data obtained from the emerging optical tomography method. These findings form the basis for future development of receptor-based optical contrast agents and could provide new approaches to the selective delivery of phototoxic agents to tumors for therapeutic interventions.

Materials and Methods

General. All reagents and solvents were obtained commercially and used without further purification. Compounds **1**, **8**, **12**−**14**, and **25** were supplied to us by our collaborator at Mallinckrodt, Inc. Purification and analysis of the dye-labeled fluorescein and carbocyanine derivatives were performed by HPLC with a tunable UV−visible detector. Analytical (flow rate = 0.5 mL/min) and semipreparative (flow rate = 10 mL/min) RP-HPLC were performed as described in the literature by using a C-18 column.[39] The gradient elution protocol ranged from a mixture of 95% A and 5% B to 30% A and 70% B in 30 min, where A is 5% MeCN in 0.1% aqueous TFA and B is 90% MeCN in 0.1% aqueous TFA. A second elution system consisting of an isocratic mixture of 60% H_2O containing 0.1% TFA, 30% MeOH, and 10% MeCN was used to confirm purity of compounds by analytical HPLC. Peak detection was at 214 nm, unless otherwise stated. Electrospray ionization mass spectrometry experiments were performed on a triple quadruple mass spectrometer. The electrospray interface was operated in positive ion mode with a spray voltage of 4.5 kV and a capillary temperature of 225 °C. Samples were introduced into the spectrometer by flow injection utilizing 70% MeCN and 30% H_2O containing 0.1% TFA. The absorption and emission spectra of the dye conjugates were performed on a Cary 500 UV−visible spectrophotometer (Varian) and QuantaMaster spectrofluorometer (Photon Technology International), respectively. High-resolution mass spectrometry (HRMS) (MALDI-TOF) analyses were performed at the Washington University School of Medicine in St. Louis, MO. The HPLC purity of all compounds used in the in vivo and in vitro studies was >99%. The dye−peptide conjugates were stable under the experimental conditions used, and no aggregation is expected at the nanomolar concentration employed in the in vitro studies.

Peptide Synthesis. All of the peptides synthesized in this study follow the procedure described below. Exceptions are noted under specific peptides. The peptides were synthesized on solid support by standard automated Fmoc procedures.[40] Rink amide and Wang resins were used for the synthesis of C-terminal amide and carboxyl peptides, respectively. Chlorotrityl resins were used for mild selective cleavage of peptides from the resin without removing the amino acids side chain protecting groups. Initial loading of each Fmoc amino acid bound resin is 25 μmol. Automatic activation of the carboxyl group with a 1:1 mixture of N-hydroxylbenzotriazole (HOBt, 2 M) and 2-(1-H benzotriazole-1-yl)-1,1,1,3-tetramethyluronium hexafluorophosphate (HBTU, 2 M) and coupling of subsequent Fmoc-protected amino acids (75 μmol) were carried out in situ. For octreotate derivatives, intramolecular cyclization of the acetamidomethyl-protected dithiol groups of cysteine was accomplished by adding thallium trifluoroacetate (23 mg, 42 μmol) in anhydrous dimethylformamide (DMF, 1 mL) and shaking the heterogeneous mixture for 2 h, followed by successive washing of the residue with water, DMF, tetrahydrofuran (THF), and DCM. Whenever applicable, incorporation of DTPA or DOTA was accomplished by placing tri-*tert*-butyl DTPA or tri-*tert*-butyl DOTA (75 μmol) in the last cartridge of amino acid rack, which is then coupled to the appropriate amino group by the same automated method used to synthesize the amino acid sequence.[41] Cleavage of the peptides from the resin and concomitant removal of the side chain protecting groups were accomplished with 85% TFA, 5% H_2O, 5% PhOH,

and 5% thioanisole for 4 h at room temperature. The crude peptides were precipitated with cold *tert*-butyl methyl ether and purified by RP-HPLC using gradient elution protocol described in the general section above. All peptides and their conjugates were characterized by analytical HPLC and electrospray spectrometric (EI) analysis after lyophilization in 67% H_2O and 33% MeCN. The nonfluorescein conjugated peptides **2**, **15**, **16**, and **26**−**28** were prepared by this procedure.

DPhe-cyclo(Cys-DTyr-Trp-Lys-Thr-Cys)Thr-OH (2). ESI-MS: m/z 1050 [M + H]$^+$, 526 [M + 2H]$^{2+}$.

Gly-Ser-Gly-Gln-Trp-Ala-Val-Gly-His-Leu-Met-NH$_2$ (15). ESI-MS: m/z 1141 [M + H]$^+$, 571 [M + 2H]$^{2+}$.

Lys-Gly-Ser-Gly-Gln-Trp-Ala-Val-Gly-His-Leu-Met-NH$_2$ (16). ESI-MS: m/z 1270 [M + H]$^+$, 636 [M + 2H]$^{2+}$.

α-DTPA-Lys-Gln-Trp-Ala-Val-Gly-His-Leu-Met-NH$_2$ (26). ESI-MS: m/z 1444 [M + H]$^+$, 723 [M + 2H]$^{2+}$, 481 [M + 3H]$^{3+}$.

ε-DTPA-Lys-Gln-Trp-Ala-Val-Gly-His-Leu-Met-NH$_2$ (27). ESI-MS: m/z 1444 [M + H]$^+$, 723 [M + 2H]$^{2+}$, 482 [M + 3H]$^{3+}$.

α,ε-(DTPA)$_2$-Lys-Gln-Trp-Ala-Val-Gly-His-Leu-Met-NH$_2$ (28). ESI-MS: m/z 910 [M + 2H]$^{2+}$, 607 [M + 3H]$^{3+}$.

Preparation Fluorescein−Peptide Conjugates by Solid Phase Synthesis. A typical example for this procedure is represented by the synthesis of the β-alanine somatostatin derivative **4**. Preparation of the peptide **2** was carried out by standard Fmoc strategy. While still on solid support and with all side chain protecting groups intact, the intramolecular cyclization of the disulfide bond was carried out with (CF$_3$-CO$_2$)$_3$Tl in DMF followed by the removal of the N-terminal Fmoc to liberate the amino group. After the resin was washed with CH$_2$Cl$_2$ (DCM), the resin was swollen in DMF for 10 min before adding Et$_3$N (10 mg, 100 μmol) and commercially available FITC (14 mg, 36 μmol). The mixture was shaken for 16 h, and the resin was washed sequentially with DMF, THF, and DCM. The product was cleaved from the resin as described above, and the resulting TFA solution was poured into cold MTBE to precipitate the yellow crude material, which was lyophilized and purified using HPLC. This procedure was used to prepare the fluorescein−nonpeptide conjugate **4** and other less sterically hindered N-terminal peptide derivatives **5** and **21**−**24**. Note that the cyclization step was omitted for all bombesin derivatives. Several attempts to prepare **3** by this method were not successful.

FITC-βAla-DPhe-cyclo(Cys-DTyr-Trp-Lys-Thr-Cys)-Thr-OH (4). ESI-MS: m/z 1510 [M + H]$^+$, 756 [M + 2H]$^{2+}$; 5 mg; 13% overall yield of isolated compound.

Preparation Fluorescein−Peptide Conjugates by Solution Phase Synthesis. Two methods were evaluated for the preparation of the bioconjugates by solution phase reaction. In the first method, the peptide was prepared on a chlorotrityl resin as described above. This resin allowed us to cleave the peptide with mild acid (5% TFA in DCM; 2 × 30 min) without removing the side chain *t*-Boc amino and *t*-Bu carboxyl side chain protecting groups on the peptide. In a typical procedure, the octapeptide **2** was cleaved from the trityl resin after cyclization and removal of N-terminal Fmoc. The crude product was precipitated with MTBE and lyophilized. Without further purification, a mixture of the orthogonally protected peptide (5 mg, 3.5 μmol), FITC (3 mg, 7 μmol), and NaHCO$_3$ (5 mg, 60 μmol) in 2 mL of DMF was shaken vigorously for 5 h. The insoluble salt was filtered, and the filtrate was precipitated and washed with MBTE (3 × 2 mL) and centrifuged, and the supernatant was decanted before lyophilization. Mass spectrometry of the crude product did not indicate a quantifiable amount of the desired compound. Coupled with the poor yield, this procedure would require extensive workup in order to remove all protecting groups and isolate the compound. Hence, this procedure was abandoned.

The second approach, which was used to prepare a majority of the conjugates, involved simultaneous cleavage of the peptide from the resin and removal of side chain protecting groups before coupling FITC to the peptide. Synthesis of the fluorescein peptide conjugate **21** is typical for the preparation of bombesin derivatives by this approach. Briefly, the peptide was prepared by standard Fmoc procedure described above

and cleaved from the resin to obtain the undecapeptide **15**. A mixture of this peptide (10 mg, 9 μmol), FITC (10 mg, 25 μmol), and NaHCO$_3$ (10 mg, 120 μmol) in 2 mL of DMF was stirred for 12 h at room temperature and filtered into cold MTBE to give a yellow-orange precipitate. The supernatant was removed after centrifugation, and the crude product was washed with MTBE (3 × 3 mL), dried, lyophilized, and purified by preparative HPLC.

In this procedure, cleavage of the somatostatin derivatives also exposes the ϵ-amino group of the lysine pharmacophore (e.g., compound **2**, K^5) to reaction with FITC. Consequently, this amino group was protected with ivDde, which is not affected by the cleavage mixture. Thus, a typical procedure for the synthesis of the somatostatin derivatives begins with the incorporation of Fmoc-lysine(ϵ-ivDde)OH in the receptor binding lysine. After the peptide synthesis was completed, cyclization and removal of the N-terminal Fmoc group and cleavage of the peptide from the resin with TFA also removed all side chain protecting groups, except ivDde. Subsequent reactions are illustrated by the synthesis of **3**. FITC (12 mg, 28 μmol) and NaHCO$_3$ (10 mg, 120 μmol) were added to a solution of the crude peptide (prepared on a 25 μmol scale) in 2 mL of DMF and stirred for 12 h. The mixture was filtered into 8 mL of MBTE to precipitate the orange product, and analysis of the crude product by HPLC showed about 50% conversion. This product was treated with a 1 mL solution of 2% hydrazine in DMF for 20 min in order to remove the ivDde. The resulting mixture was poured into cold MBTE to precipitate the conjugate, which was lyophilized and purified by HPLC.

A similar method was used to prepare the bombesin peptide derivatives, except that the cyclization step was not required. Because the receptor binding region of bombesin peptides are devoid of lysine residue, orthogonal protection of the amino groups with ivDde was only required when a lysine linker was involved. On the basis of the FITC coupling reaction step, the isolated yield in all cases ranged from 20 to 25% of the expected yield.

FITC-DPhe-cyclo(Cys-DTyr-Trp-Lys-Thr-Cys)Thr-OH (3). ESI-MS: *m/z* 1438 [M + H]$^+$, 720 [M + 2H]$^{2+}$.

FITC-Gly-Ser-Gly-DPhe-cyclo(Cys-DTyr-Trp-Lys-Thr-Cys)Thr-OH (5). ESI-MS: *m/z* 1640 [M + H]$^+$, 821 [M + 2H]$^{2+}$.

α-FITC-Lys-DPhe-cyclo(Cys-DTyr-Trp-Lys-Thr-Cys)-Thr-OH (6). To specifically prepare this compound, the ϵ-amino group of both K^1 and K^6 was protected with ivDde, which remained intact after peptide cleavage from the resin with TFA. This guarantees that only the α-amino group of N-terminal lysine reacts with FITC. Subsequent removal of the ivDde protecting group was carried out with 2% hydrazine in DMF, as described above. ESI-MS: *m/z* 1567 [M + H]$^+$, 784 [M + 2H]$^{2+}$, 523 [M + 3H]$^{3+}$.

ϵ-FITC-Lys-DPhe-cyclo(Cys-DTyr-Trp-Lys-Thr-Cys)-Thr-OH (7). To ensure the coupling of FITC to the ϵ-position, the reaction was carried out as described for compound **6** above, except that the α-amino group of K^1 was protected with ivDde. ESI-MS: *m/z* 1567 [M + H]$^+$, 784 [M + 2H]$^{2+}$, 523 [M + 3H]$^{3+}$.

α-DTPA-ϵ-FITC-Lys-DPhe-cyclo(Cys-DTyr-Trp-Lys-Thr-Cys)Thr-OH (9). In this reaction, the ϵ-amino group of K^6 was protected as ivDde while Fmoc-Lys(Boc) was used for the N-terminal amino group. Thus, at the end of the peptide synthesis, tri-*tert*-butyl DTPA was directly coupled to the α-amino group of K^1 after Fmoc removal. Cleavage of the peptide from the resin with TFA also removed the Boc group, which allowed us to introduce FITC at the ϵ-amino position. ESI-MS: *m/z* 1942 [M + H]$^+$, 972 [M + 2H]$^{2+}$, 648 [M + 3H]$^{3+}$.

α-FITC-ϵ-DTPA-Lys-DPhe-cyclo(Cys-DTyr-Trp-Lys-Thr-Cys)Thr-OH (10). A similar method described for compound **9** was used except that Boc-Lys(Fmoc) was used for the N-terminal lysine. ESI-MS: *m/z* 1942 [M + H]$^+$, 972 [M + 2H]$^{2+}$, 648 [M + 3H]$^{3+}$.

α-DOTA-ϵ-FITC-Lys-DPhe-cyclo(Cys-DTyr-Trp-Lys-Thr-Cys)Thr-OH (11). A similar method described for compound

9 was used except that tri-*tert*-butyl DOTA instead of tri-*tert*-butyl DTPA was used as the chelating group. ESI-MS: *m/z* 1953 [M + H]$^+$, 977 [M + 2H]$^{2+}$, 652 [M + 3H]$^{3+}$.

FITC-Gln-Trp-Ala-Val-Gly-His-Leu-Met-NH$_2$ (17). ESI-MS: *m/z* 1330 [M + H]$^+$, 666 [M + 2H]$^{2+}$.

α-FITC-Lys-Gln-Trp-Ala-Val-Gly-His-Leu-Met-NH$_2$ (18). To ensure selective coupling of FITC to the α-position, Fmoc-Lys(ivDde) was used to prepare this compound by the procedure described for the synthesis of compound **6**. ESI-MS: *m/z* 1458 [M + H]$^+$, 730 [M + 2H]$^{2+}$, 487 [M + 3H]$^{3+}$.

ϵ-FITC-Lys-Gln-Trp-Ala-Val-Gly-His-Leu-Met-NH$_2$ (19). Conjugation of FITC to the ϵ-position was assured by using ivDde-Lys(ivDde) by the procedure described for the synthesis of compound **6**. ESI-MS: *m/z* 1458 [M + H]$^+$, 730 [M + 2H]$^{2+}$, 487 [M + 3H]$^{3+}$.

α,ϵ-(FITC)$_2$-Lys-Gln-Trp-Ala-Val-Gly-His-Leu-Met-NH$_2$ (20). ESI-MS: *m/z* 1846 [M + H]$^+$, 924 [M + 2H]$^{2+}$, 616 [M + 3H]$^{3+}$.

FITC-Gly-Ser-Gly-Gln-Trp-Ala-Val-Gly-His-Leu-Met-NH$_2$ (21). ESI-MS: *m/z* 1532 [M + H]$^+$, 766 [M + 2H]$^{2+}$.

α-FITC-Lys-Gly-Ser-Gly-Gln-Trp-Ala-Val-Gly-His-Leu-Met-NH$_2$ (22). ESI-MS: *m/z* 1659 [M + H]$^+$, 830 [M + 2H]$^{2+}$, 554 [M + 3H]$^{3+}$.

ϵ-FITC-Lys-Gly-Ser-Gly-Gln-Trp-Ala-Val-Gly-His-Leu-Met-NH$_2$ (23). ESI-MS: *m/z* 1660 [M + H]$^+$, 830 [M + 2H]$^{2+}$, 554 [M + 3H]$^{3+}$.

α,ϵ-(FITC)$_2$-Lys-Gly-Ser-Gly-Gln-Trp-Ala-Val-Gly-His-Leu-Met-NH$_2$ (24). ESI-MS: *m/z* 1025 [M + 2H]$^{2+}$, 684 [M + 3H]$^{3+}$.

α-DTPA-ϵ-FITC-Lys-Gln-Trp-Ala-Val-Gly-His-Leu-Met-NH$_2$ (29). ESI-MS: *m/z* 1833 [M + H]$^+$, 918 [M + 2H]$^{2+}$, 612 [M + 3H]$^{3+}$.

α-FITC-ϵ-DTPA-Lys-Gln-Trp-Ala-Val-Gly-His-Leu-Met-NH$_2$ (30). ESI-MS: *m/z* 1833 [M + H]$^+$, 918 [M + 2H]$^{2+}$, 612 [M + 3H]$^{3+}$.

α-FITC-ϵ-DOTA-Lys-Gln-Trp-Ala-Val-Gly-His-Leu-Met-NH$_2$ (31). ESI-MS: *m/z* 1845 [M + H]$^+$, 923 [M + 2H]$^{2+}$, 615 [M + 3H]$^{3+}$.

Synthesis of Peptide−Tricarbocyanine-*bis*-propanoic Acid Derivatives (32, 35, 36). A mixture of 1,1,2-trimethyl-[1H]-benz[*e*]indole **37** (9.1 g, 43.58 mmol) and 3-bromopropanoic acid (10.0 g, 65.37 mmol) in 1,2-dichlorobenzene (40 mL) was heated at 110 °C for 12 h. The solution was cooled to room temperature, and the residue obtained was filtered and washed with a mixture of acetonitrile/diethyl ether (1/1). The solid obtained was dried under vacuum to give 10 g (64%) of light brown powder. A portion of this solid (6.0 g, 16.56 mmol) was added to a mixture of glutaconaldehyde dianil monohydrochloride (2.36 g, 8.28 mmol) and sodium acetate trihydrate (2.93 g, 21.53 mmol) in 150 mL of ethanol, and the resulting heterogeneous mixture was heated at reflux for 90 min. After the solvent was evaporated, the residue was washed with 2 M aqueous HCl (4 × 40 mL) and the green paste obtained was lyophilized in water/MeCN (3/2) to give dark green flakes (2 g, 35% yield; ESI-MS: *m/z* 625.3 [M + H]$^+$.

While still on solid support, the N-terminal Fmoc group of the peptide was removed and washed with 3 mL each of DMF, MeOH, THF, and DCM in that order. The resin-bound peptide was added to preactivated carbocyanine dye **39** (53 mg, 75 mmol; activated with 80 mmol of HBTU in DMSO for 30 min). After the reaction mixture was shaken for 3 h, the resin was washed with DMF and DCM, followed by peptide cleavage and removal of side chain protecting groups with a mixture of 85% TFA, 7.5% H$_2$O, and 7.5% thioanisole in 4 h. The peptide−dye conjugate was precipitated from the cleavage mixture with cold MTBE and lyophilized in MeCN/H$_2$O (2/3) mixture. The green crude product was purified by HPLC as described in the General Section to give the cytate in 99% HPLC purity.

Tricarbocyanine-DPhe-cyclo(Cys-DTyr-Trp-Lys-Thr-Cys)Thr-OH (32). ESI-MS: *m/z* 1656 [M + H]$^+$, 829 [M + 2H]$^{2+}$.

Tricarbocyanine-βAla-DPhe-cyclo(Cys-DTyr-Trp-Lys-Thr-Cys)Thr-OH (35). ESI-MS: *m/z* 1728 [M + H]$^+$, 864 [M + 2H]$^{2+}$.

Tricarbocyanine-Gly-Ser-Gly-Gln-Trp-Ala-Val-Gly-His-Leu-Met-NH₂ (36). ESI-MS: m/z 1748 [M + H]⁺, 875 [M + 2H]²⁺.

Synthesis of Peptide−Tricarbocyanine-*bis*-hexanoic Acid Derivatives (33, 34). A similar procedure described above was used to prepare these compounds except that 1,1,2-trimethyl-[1H]-benz[*e*]indole **37** was reacted with 6-bromohexanoic acid instead of 3-bromopropanoic acid to give the intermediate 1,1,2-trimethyl-[1H]-benz[*e*]indole-*N*-hexanoic acid. Reaction of this intermediate (4 g, 9.89 mmol) with glucaconaldehyde dianil hydrochloride (1.4 g, 4.95 mmol) as described above gave the carbocyanine dye **39** (with hexanaoic instead of propanoic acid *N*-alkyl derivative, 1.8 g, 46% yield; ESI-MS: m/z 709.4 [M + H]⁺). This dye was used to prepare the peptide conjugates **33** and **34**.

Tricarbocyanine-DPhe-cyclo(Cys-DTyr-Trp-Lys-Thr-Cys)Thr-OH (33). ESI-MS: m/z 1740 [M + H]⁺, 871 [M + 2H]²⁺, 581 [M + 3H]³⁺.

Tricarbocyanine(DPhe-cyclo(Cys-DTyr-Trp-Lys-Thr-Cys)Thr-OH)₂ (34). ESI-MS: m/z 1387 [M + 2H]²⁺, 925 [M + 3H]³⁺.

In Vitro Receptor Binding Assays. Receptor binding assays were performed using membranes prepared from the rat pancreatic acinar cell lines AR42-J and CA20948 for bombesin and somatostatin receptor binding assays, respectively. Membranes were prepared by a method similar to that previously reported.[30] Assays were carried out using Millipore FC96 plates and the Millipore Multiscreen system (Bedford, MA). For bombesin derivatives, the competitive receptor binding of the tracer [¹¹¹In]-DTPA-[P¹,Y⁴]-bombesin to AR42-J cell membranes (~50 µg/well) was determined in the presence of increasing concentration of cold competitors in buffer (50 mM Tris-HCl, pH 7.4, 5 mM MgCl₃, 0.2 mg/mL BSA) in a total volume of 200 µL per well. Similarly, somatostatin receptor binding studies used the tracer [¹¹¹In]-DTPA-[Y³]-octreotate and CA20948 cell membranes (~25 mg/well). Following incubation for 90 min at room temperature, membranes were filtered and washed with buffer. The filters containing membrane-bound radioactivity were removed from the assay plate and counted using a Parkard Cobra gamma counter (Meriden, CT). IC₅₀ values were calculated using a four parameter curve-fitting routine using the program GraFit (Erithacus Software, U.K.). Radiolabeling of DTPA-linked peptides was carried out in 25 mM NaOAc and 12.5 mM sodium ascorbate (pH 5.0, room temperature, 30 min incubation). The specific activity of radiolabeled peptides was >1400 Ci/mmol. Radiochemical yield (>99.5%) and radiochemical purity (>98%) were determined by reverse phase chromatography on a C18 Vydac column using a MeCN/0.1% TFA gradient (5−70% MeCN over 20 min) at a flow rate of 1 mL/min. Binding assays were performed in duplicates per sample, and the experiment was repeated twice. The stock solutions of dye-labeled peptides were prepared by adding an accurate amount of the weighed bioconjugate to 25% DMSO in water, and other concentrations were obtained by serial dilution of aliquots from the stock.

Animal Protocols. All studies were conducted in compliance with Mallinckrodt Inc. Animal Welfare Committee's requirements for the care and use of laboratory animals in research. The rat pancreatic acinar carcinoma (CA20948) expressing the somatostatin receptor was induced by solid implant technique in the rear left flank area. Palpable masses were detected 9 days postimplant. This tumor line has been widely used for somatostatin receptor-positive assays, and the number of binding sites for somatostatin is estimated at 489 fmol mg⁻¹.[48]

The animals were anesthetized with a rat cocktail (xylazine:ketamine:acepromazine 1.5:1.5:0.5) at 0.8 mL/kg via intaperitoneal injection. The area of the tumor (left flank) was shaved to expose the tumor and surrounding surface area. A 21 gauge butterfly infusion set equipped with a stopcock and two syringes containing heparinized saline was placed into the lateral tail vein of the rat. Patency of the vein was checked prior to administration of the new contrast agents via the butterfly apparatus. Each animal weighing about 250 g received 0.5 mL of aqueous solution of ICG (5.4 µM) or cytate (6.0 µM).

Imaging Procedure. A simple noninvasive in vivo continuous wave fluorescence imaging apparatus employed to assess the localization and distribution of contrast agents has been previously described.[27,29] Briefly, laser light of the appropriate incident wavelength to excite the agent fluorescence was launched into a fiber optic bundle. A defocusing lens in position after the bundle expanded the beam such that most of the rat was illuminated. An argon ion laser tuned to 488 nm was used to excite the fluorescein compounds, and a 780 nm laser diode was used for the carbocyanine compounds. The lasers generated a nominal 50 mW of incident power. The laser power at the output of the bundle was approximately one-half of the input power.

The detector was a Princeton Instruments CCD camera. An interference filter in front of the CCD (520 nm for fluorescein compounds and 830 nm for carbocyanine compounds) allowed for detection of the emitted fluorescent light only. Images were acquired and processed using WinView software from Princeton Instruments. Typically, an image of the animal was taken preadministration of contrast agent. Subsequent images were taken post administration of the agent, all performed with the rat in a stationary position. Data analysis consisted of subtracting (pixel by pixel) the preadministration image from the postadministration images and displaying the results in gray scale or false color. For images taken several hours postadministration, the animals were removed from the sample area, returned to their habitat, and then brought back to the sample area. Background subtraction was not performed for these measurements.

References

(1) Shah, N.; Cerussi, A.; Eker, C.; Espinoza, J.; Butler, J.; et al. Noninvasive functional optical spectroscopy of human breast tissue. *Proc. Natl. Acad. Sci. U.S.A.* **2001**, *98*, 4420−4425.

(2) Hawrysz, D. J.; Sevick-Muraca, E. M. Developments toward diagnostic breast cancer imaging using near-infrared optical measurements and fluorescent contrast agents. *Neoplasia* **2000**, *2*, 388−417.

(3) Cheong, W. F.; vanHouten, J. P.; Kermit, E. L.; Machold, T. R.; Stevenson, D. K.; et al. Pilot comparison of light-based optical tomography versus ultrasound for real-time imaging of neonatal intraventricular hemorrhage. *Pediatr. Res.* **1996**, *39*, 1189−1189.

(4) Rhine, W. D.; Benaron, D. A.; Darceuil, H. E.; deCrespigny, A.; Cheong, W. F.; et al. Simultaneous time of-flight adjusted (TOFA) near-infrared spectroscopy and magnetic resonance imaging of immature rabbit hypoxic-ischemic encephalopathy (HIE). *Pediatr. Res.* **1996**, *39*, 2264−2264.

(5) Wagnieres, G. A.; Star, W. M.; Wilson, B. C. In vivo fluorescence spectroscopy and imaging for oncological applications. *Photochem. Photobiol.* **1998**, *68*, 603−632.

(6) Ntziachristos, V.; Yodh, A. G.; Schnall, M.; Chance, B. Concurrent MRI and diffuse optical tomography of breast after indocyanine green enhancement. *Proc. Natl. Acad. Sci. U.S.A.* **2000**, *97*, 2767−2772.

(7) Cubeddu, R.; Pifferi, A.; Taroni, P.; Torricelli, A.; Valentini, G.; et al. Fluorescence imaging during photodynamic therapy of experimental tumors in mice sensitized with disulfonated aluminum phthalocyanine. *Photochem. Photobiol.* **2000**, *72*, 690−695.

(8) Cerussi, A. E.; Berger, A. J.; Bevilacqua, F.; Shah, N.; Jakubowski, D.; et al. Sources of absorption and scattering contrast for near-infrared optical mammography. *Acad. Radiol.* **2001**, *8*, 211−218.

(9) Hebden, J. C.; Veenstra, H.; Dehghani, H.; Hillman, E. M. C.; Schweiger, M.; et al. Three-dimensional time-resolved optical tomography of a conical breast phantom. *Appl. Opt.* **2001**, *40*, 3278−3287.

(10) Culver, J. P.; Ntziachristos, V.; Holboke, M. J.; Yodh, A. G. Optimization of optode arrangements for diffuse optical tomography: A singular-value analysis. *Opt. Lett.* **2001**, *26*, 701−703.

(11) Hyde, D. E.; Farrell, T. J.; Patterson, M. S.; Wilson, B. C. A diffusion theory model of spatially resolved fluorescence from depth-dependent fluorophore concentrations. *Phys. Med. Biol.* **2001**, *46*, 369−383.

(12) Pogue, B. W.; Geimer, S.; McBride, T. O.; Jiang, S. D.; Osterberg, U. L.; et al. Three-dimensional simulation of near-infrared diffusion in tissue: boundary condition and geometry analysis for finite- element image reconstruction. *Appl. Opt.* **2001**, *40*, 588−600.

(13) McBride, T. O.; Pogue, B. W.; Gerety, E. D.; Poplack, S. B.; Osterberg, U. L.; et al. Spectroscopic diffuse optical tomography for the quantitative assessment of hemoglobin concentration and oxygen saturation in breast tissue. *Appl. Opt.* **1999**, *38*, 5480–5490.

(14) Schotland, J. C. Continuous-wave diffusion imaging. *J. Opt. Soc. Am. A* **1997**, *14*, 275–279.

(15) Lee, J.; Sevick-Muraca, E. Fluorescence-enhanced absorption imaging using frequency-domain photon migration: tolerance to measurement error. *J. Biomed. Opt.* **2001**, *6*, 58–67.

(16) Katzenellenbogen, J. A.; Coleman, R. E.; Hawkins, R. A.; Krohn, K. A.; Larson, S. M.; et al. Tumor receptor imaging: Proceedings of the national cancer institute workshop, review of current work, and prospective for further investigations. *Clin. Cancer Res.* **1995**, *1*, 921–932.

(17) Clauss, M. A.; Jain, R. K. Interstitial Transport of Rabbit and Sheep Antibodies in Normal and Neoplas Tic Tissues. *Cancer Res.* **1990**, *50*, 3487–3492.

(18) Pelegrin, A.; Folli, S.; Buchegger, F.; Mach, J. P.; Wagnieres, G.; et al. Antibody Fluorescein Conjugates for Photoimmunodiagnosis of Human Colon-Carcinoma in Nude-Mice. *Cancer* **1991**, *67*, 2529–2537.

(19) Vogel, C. A.; Galmiche, M. C.; Westermann, P.; Sun, L. Q.; Pelegrin, A.; et al. Carcinoembryonic antigen expression, antibody localisation and immunophotodetection of human colon cancer liver metastases in nude mice: A model for radioimmunotherapy. *Int. J. Cancer* **1996**, *67*, 294–302.

(20) Folli, S.; Westermann, P.; Braichotte, D.; Pelegrin, A.; Wagnieres, G.; et al. Antibody-Indocyanin Conjugates for Immunophotodetection of Human Squamous-Cell Carcinoma in Nude-Mice. *Cancer Res.* **1994**, *54*, 2643–2649.

(21) Ballou, B.; Fisher, G. W.; Deng, J. S.; Hakala, T. R.; Srivastava, M.; et al. Cyanine fluorochrome-labeled antibodies in vivo: Assessment of tumor imaging using Cy3, Cy5, Cy5.5, and Cy7. *Cancer Detect. Prev.* **1998**, *22*, 251–257.

(22) Ballou, B.; Fisher, G. W.; Hakala, T. R.; Farkas, D. L. Tumor detection and visualization using cyanine fluorochrome-labeled antibodies. *Biotechnol. Prog.* **1997**, *13*, 649–658.

(23) Ballou, B.; Fisher, G. W.; Waggoner, A. S.; Farkas, D. L.; Reiland, J. M.; et al. Tumor Labeling in-Vivo Using Cyanine-Conjugated Monoclonal- Antibodies. *Cancer Immunol. Immunother.* **1995**, *41*, 257–263.

(24) Becker, A.; Riefke, B.; Ebert, B.; Sukowski, U.; Rinneberg, H.; et al. Macromolecular contrast agents for optical imaging of tumors: Comparison of indotricarbocyanine-labeled human serum albumin and transferrin. *Photochem. Photobiol.* **2000**, *72*, 234–241.

(25) Bremer, C.; Tung, C. H.; Weissleder, R. In vivo molecular target assessment of matrix metalloproteinase inhibition. *Nat. Med.* **2001**, *7*, 743–748.

(26) Tung, C. H.; Bredow, S.; Mahmood, U.; Weissleder, R. Preparation of a cathepsin D sensitive near-infrared fluorescence probe for imaging. *Bioconjugate Chem.* **1999**, *10*, 892–896.

(27) Achilefu, S.; Dorshow, R. B.; Bugaj, J. E.; Rajagopalan, R. Novel receptor-targeted fluorescent contrast agents for in vivo tumor imaging. *Invest. Radiol.* **2000**, *35*, 479–485.

(28) Becker, A.; Hessenius, C.; Licha, K.; Ebert, B.; Sukowski, U.; et al. Receptor-targeted optical imaging of tumors with near-infrared fluorescent ligands. *Nat. Biotechnol.* **2001**, *19*, 327–331.

(29) Bugaj, J. E.; Achilefu, S.; Dorshow, R. B.; Rajagopalan, R. Novel fluorescent contrast agents for optical imaging of in vivo tumors based on a receptor-targeted dye-peptide conjugate platform. *J. Biomed. Opt.* **2001**, *6*, 122–133.

(30) Raynor, K.; Reisine, T. Analogues of Somatostatin Selectively Label Distinct Subtypes of Somatostatin Receptors in Rat-Brain. *J. Pharmacol. Exp. Ther.* **1989**, *251*, 510–517.

(31) Reubi, J. C.; Waser, B.; Schaer, J. C.; Laissue, J. A. Somatostatin receptor sst1-sst5 expression in normal and neoplastic human tissues using receptor autoradiography with subtype-selective ligands. *Eur. J. Nucl. Med.* **2001**, *28*, 836–846.

(32) Behr, T. M.; Gotthardt, M.; Barth, A.; Behe, M. Imaging tumors with peptide-based radioligands. *Q. J. Nucl. Med.* **2001**, *45*, 189–200.

(33) Janson, E. T.; Westlin, J. E.; Ohrvall, U.; Oberg, K.; Lukinius, A. Nuclear localization of In-111 after intravenous injection of [In-111-DTPA-D-Phe(1)]-octreotide in patients with neuroendocrine tumors. *J. Nucl. Med.* **2000**, *41*, 1514–1518.

(34) Lewis, J. S.; Srinivasan, A.; Schmidt, M. A.; Anderson, C. J. In vitro and in vivo evaluation of Cu-64-TETA-Tyr(3)- octreotate. A new somatostatin analogue with improved target tissue uptake. *Nucl. Med. Biol.* **1999**, *26*, 267–273.

(35) Hoffman, T. J.; Quinn, T. P.; Volkert, W. A. Radiometalated receptor-avid peptide conjugates for specific in vivo targeting of cancer cells. *Nucl. Med. Biol.* **2001**, *28*, 527–539.

(36) Glasspool, R. M.; Evans, T. R. J. Clinical imaging of cancer metastasis. *Eur. J. Cancer* **2000**, *36*, 1661–1670.

(37) Hintz, S. R.; Cheong, W. F.; Van Houten, J. P.; Stevenson, D. K.; Benaron, D. A. Bedside imaging of intracranial hemorrhage in the neonate using light: Comparison with ultrasound, computed tomography, and magnetic resonance imaging. *Pediatr. Res.* **1999**, *45*, 54–59.

(38) Chang, J. W.; Graber, H. L.; Koo, P. C.; Aronson, R.; Barbour, S. L. S.; et al. Optical imaging of anatomical maps derived from magnetic resonance images using time-independent optical sources. *IEEE Trans. Med. Imaging* **1997**, *16*, 68–77.

(39) Edwards, W. B.; Fields, C. G.; Anderson, C. J.; Pajeau, T. S.; Welch, M. J.; et al. Generally Applicable, Convenient Solid-Phase Synthesis and Receptor Affinities of Octreotide Analogues. *J. Med. Chem.* **1994**, *37*, 3749–3757.

(40) Atherton, E.; Sheppard, R. C. *Solid Phase Peptide Synthesis: A Practical Appraoch*; Oxford University Press: Oxford, England, 1989.

(41) Achilefu, S.; Wilhelm, R. R.; Jimenez, H. N.; Schmidt, M. A.; Srinivasan, A. A new method for the synthesis of tri-*tert*-butyl diethylenetriaminepentaacetic acid and its derivatives. *J. Org. Chem.* **2000**, *65*, 1562–1565.

(42) Packard, B. Z.; Komoriya, A.; Toptygin, D. D.; Brand, L. Structural characteristics of fluorophores that form intramolecular H-type dimers in a protease substrate. *J. Phys. Chem. B* **1997**, *101*, 5070–5074.

(43) Reichert, D. E.; Welch, M. J. Applications of molecular mechanics to metal-based imaging agents. *Coord. Chem. Rev.* **2001**, *212*, 111–131.

(44) de Jong, M.; Breeman, W. A. P.; Bernard, B. F.; Bakker, W. H.; Schaar, M.; et al. [Lu-177-DOTA(0), Tyr(3)]octreotate for somatostatin receptor- targeted radionuclide therapy. *Int. J. Cancer* **2001**, *92*, 628–633.

(45) Karra, S. R.; Schibli, R.; Gali, H.; Katti, K. V.; Hoffman, T. J.; et al. Tc-99m-labeling and in vivo studies of a bombesin analogue with a novel water-soluble dithiadiphosphine-based bifunctional chelating agent. *Bioconjugate Chem.* **1999**, *10*, 254–260.

(46) Ntziachristos, V.; Chance, B. Probing physiology and molecular function using optical imaging: applications to breast cancer. *Breast Cancer Res.* **2001**, *3*, 41–46.

(47) Ferone, D.; Kwekkeboom, D. J.; Pivonello, R.; Bogers, A.; Colao, A.; et al. In vivo and in vitro expression of somatostatin receptors in two human thymomas with similar clinical presentation and different histological features. *J. Endocrinol. Invest.* **2001**, *24*, 522–528.

(48) Stolz, B.; Weckbecker, G.; Smith-Jones, P. M.; Albert, R.; Raulf, F.; et al. The somatostatin receptor-targeted radiotherapeutic [Y-90-DOTA- DPhe(1), Tyr(3)]octreotide (Y-90-SMT 487) eradicates experimental rat pancreatic CA 20948 tumours. *Eur. J. Nucl. Med.* **1998**, *25*, 668–674.